The monopulsed nature of sperm whale clicks

Bertel Møhl,[a] Magnus Wahlberg, and Peter T. Madsen[b]
Department of Zoophysiology, Institute of Biological Sciences, University of Aarhus, DK-8000 Aarhus C, Denmark

Anders Heerfordt
Computer Sciences, Corporation Scandinavia, Retortvej 8, DK-1780 V, Copenhagen, Denmark

Anders Lund
Department of Animal Behaviour, Zoological Institute, University of Copenhagen, Tagensvej 16, DK-2200 N, Denmark

(Received 12 August 2002; revised 14 December 2002; accepted 15 April 2003)

Traditionally, sperm whale clicks have been described as multipulsed, long duration, nondirectional signals of moderate intensity and with a spectrum peaking below 10 kHz. Such properties are counterindicative of a sonar function, and quite different from the properties of dolphin sonar clicks. Here, data are presented suggesting that the traditional view of sperm whale clicks is incomplete and derived from off-axis recordings of a highly directional source. A limited number of assumed on-axis clicks were recorded and found to be essentially monopulsed clicks, with durations of 100 μs, with a composite directionality index of 27 dB, with source levels up to 236 dB *re*: 1 μPa (rms), and with centroid frequencies of 15 kHz. Such clicks meet the requirements for long-range biosonar purposes. Data were obtained with a large-aperture, GPS-synchronized array in July 2000 in the Bleik Canyon off Vesterålen, Norway (69°28′ N, 15°40′ E). A total of 14 h of sound recordings was collected from five to ten independent, simultaneously operating recording units. The sound levels measured make sperm whale clicks by far the loudest of sounds recorded from any biological source. On-axis click properties support previous work proposing the nose of sperm whales to operate as a generator of sound.
[DOI: 10.1121/1.1586258]

PACS numbers: 43.80.Ka, 43.64.Tk, 43.30.Vh [WA]

I. INTRODUCTION

Since the first detailed description of the properties of sperm whale clicks by Backus and Schevill (1966), the unique, multipulsed nature of these clicks has been their ''trademark:'' regularly spaced pulses of sound of a few ms duration and with a decreasing amplitude. The interpulse interval (IPI) is on the order of 5 ms, and three or more pulses may be found in a click. Thus, the duration of a click may reach 20 to 30 ms (see Fig. 1).

Early investigators of sperm whale clicks (Backus and Schevill, 1966; Dunn, 1969; Levenson, 1974; Watkins, 1980) reported source levels to be moderate (170–180 dB *re*: 1 μPa), directionality to be low or absent, and the spectrum of the clicks to peak in the 2- to 8-kHz range. However, studies using large-aperture array techniques found source levels between 202 and 223 dB *re*: 1 μPa, a pronounced directionality and spectral emphasis above 10 kHz, as documented in part or all of the following papers: Whitney, 1968; Madsen and Møhl, 2000; Møhl *et al.*, 2000; Thode *et al.*, 2002. Thus, two views on the properties of sperm whale clicks may be said to exist, in the following referred to as the classical view and the large-aperture view, respectively. The present work, using a specially designed array, quantitatively extends the large-aperture view.

The multipulsed nature of sperm whale clicks inspired the dominating theory of sound production mechanics in this whale by Norris and Harvey (1972), explaining the interpulse interval (IPI) of the click by quantitative properties of the nasal anatomy: the length of the spermaceti organ, the velocity of sound in spermaceti, and the distance between the sound-reflecting air sacs at each end of the spermaceti organ. A single pulse, possibly generated by the monkey lips (a massive valve-like structure in the right nasal passage) at the front of the spermaceti organ, was proposed to initiate each click. The multipulsed click was seen as the result of reverberation of the initial pulse between the two air sacs. For each reverberation, as well as from the initial pulse, a part of the sound energy would exit to the water. This was indeed a bold proposal since the nose of sperm whales, responsible for the characteristic, box-shaped appearance of the head, makes up about 1/3 of the total body length, the latter being on the order of 15 meters in adult males. However, the anatomy and basic mechanisms of the supracranial soft anatomy are considered homologous to that found in other, smaller odontocetes (Cranford *et al.*, 1996). Here, a sound-generating function for these tissues is well established.

The Norris and Harvey scheme has recently been supported by sound-transmission experiments within the spermaceti complex (Møhl, 2001; Møhl *et al.*, 2003; Madsen *et al.*, 2003). The scheme is the theory behind acoustic remote sizing of sperm whales, exploiting that the interpulse interval is a function of the length of the spermaceti organ,

[a]Electronic mail: bertel.moehl@biology.au.dk
[b]Present address: The Ocean Alliance/The Whale Conservation Institute, 191 Weston Road, Lincoln, MA 01775.

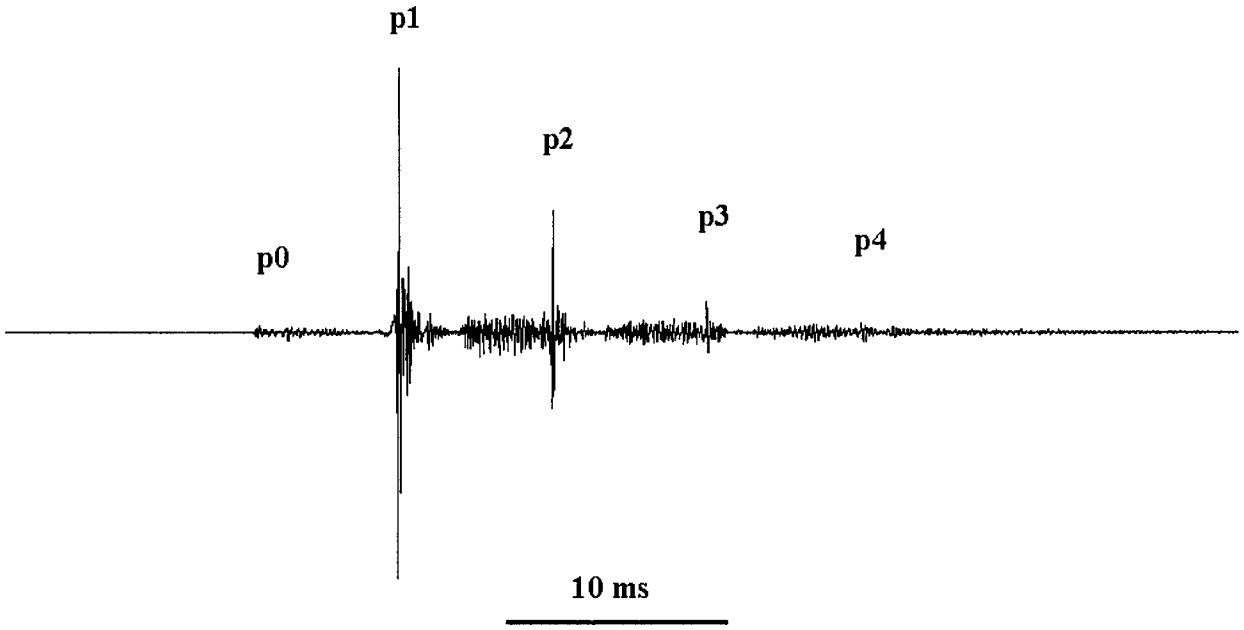

FIG. 1. The classical, multipulse structure of a sperm whale click with pulses labeled from p0 and upwards. The term ''N&H set'' (Norris and Harvey set) is proposed to signify the set of uniformly spaced pulses with decaying amplitude. The p0 pulse has special properties and significance, but is included in the concept of the N&H set. (Surface-reflected pulses of p1 to p3 have been suppressed by editing).

which again is a function of the total body length (Gordon, 1991).

Since the properties of sperm whale clicks, according to the classical view, are quite different from the biosonar clicks known from other odontocetes, it is hardly surprising that little agreement is found in the literature on the function of sperm whale clicks.[1] Norris and Harvey suggested that the multipulsed nature of the clicks would be an advantage for sonar in a cluttered environment, giving the echoes a ''mushy'' appearance. This conjecture seems to be in conflict with accepted theories on sonar (Urick, 1983). Watkins (1980) finds the sonar function less likely, based on the observations of the long duration of clicks, lack of directionality, and his experience that only whales in contact with each other seemed to click. Thus, he favors a communication function of the clicks. In contrast, Goold and Jones (1995) favor the sonar function. They estimate the theoretical detection range of 680 m for a squid target (*Loligo*), based on a specified set of assumptions. Recently, Fristrup and Harbison (2002) pursued the same line of reasoning based on the same (classical) data, but they reached the opposite conclusion, namely that sperm whale clicks are not suited for the detection of cephalopod prey. Finally, Cranford (1999) and Gordon (in Goold and Jones, 1995) see the multipulsed click pattern as a means of signaling size to conspecifics, and conjecture that females prefer mating with males with large IPI.

Our view is that sperm whale usual clicks have a sonar function, and that the multipulsed character of sperm whale clicks is derived from off-axis recordings, which give a distorted representation of the salient properties of the highly directional clicks. Off-axis recordings are not suited for evaluation of the sonar detection range of relevance to the whale. Instead, we hold the trademark of sperm whale clicks (when recorded on axis) to be monopulsed, having an extremely high intensity and directionality. A practical drawback of this trademark is the inherent difficulties to observe on-axis signals. This paper presents evidence for the monopulse click, as well as requirements and methods for obtaining such evidence. We also discuss how this concept relates to the anatomy of the sperm whale nose and to the Norris and Harvey (1972) scheme, as well as the implications of the monopulse click used as a biosonar signal.

II. MATERIAL AND METHODS

A. Environmental conditions

Data were obtained off Andenes, Norway in the period from 12 July to 25 July 2000. Here, an undersea canyon in the continental shelf forms a deep-water gully 18 km from shore. Male, adult sperm whales with a mean length of about 15 m (Wahlberg *et al.*, 1995) abound in this canyon during summer and form the basis of whale safari operations (Ciano and Huerle, 2001), as well as for sound recording operations (Møhl *et al.*, 2000). These waters are part of the Norwegian Coastal Current, running NE at about 1 knot. The velocity of sound decreases gradually with depth from 1477 m/s at the surface to 1468 m/s at 500-m depth, with little further change till the seafloor. The shape of the sound velocity profile agreed with measurements done during previous years (Fig. 2 in Wahlberg *et al.*, 2001).

1. Overview

The recordings were made with an array of up to 10 hydrophones, deployed from 7 vessels (4 yachts, ranging from 12 to 44 tons, and 3 zodiacs). The principles of this array are described in Møhl *et al.* (2001). Basically, each vessel continuously logs its position and time stamps on one track of a DAT recorder, the other track being used for sound recordings. Position and time is obtained from a Garmin 25 GPS receiver, augmented with a dGPS receiver (Magellan

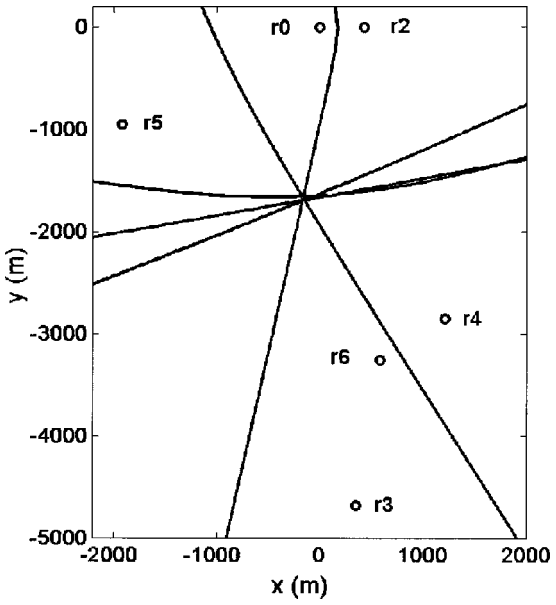

FIG. 2. Example of the recording geometry in 2D format. Relative positions of hydrophones (r0–r6) are marked with circles. Differences in time of arrival of a sperm whale click on pairs of hydrophones are used to generate hyperboloid surfaces, intercepting at the location of the source. Derived sound levels at 1 m from the source of this particular click on hydrophones r3, r6, and r4 were 193, 234, and 185 dB re: 1 μPa peRMS, respectively.

DBR IV beacon receiver), which brings positional uncertainties down to 2.5 m at the 95% level. The position (latitude–longitude format, WGS84 datum), time stamp, and other digital information (see below) are converted to an analog signal by FSK (frequency shift keying) modulation. Each time stamp is in HH:MM:SS UTC format and is recorded as a labeled time marker each second, with a precision limited by the time resolution of the DAT recorder (about 50 μ s). This technique differs from the one used by Møhl *et al.* (2000) by dispensing with synchronization by radio links. Consequently, radio noise is eliminated and the dynamic range is increased. Each node in the array is independent of the other nodes. The other digital information recorded includes tape log information keyed in by the operator, such as positional offset between the hydrophone and the GPS-antenna, sea state, surface activity of whales, attenuator settings, etc., along with the full set of the NMEA sentences generated by the Garmin receiver. The content of the tapes is subsequently transferred to compact disks (CD), preserving the original digitization and linkage between recorded sound, position, time stamps, and tape log information.

With knowledge of sound velocity in water, this array allows for tracking of the sonically active whales in three dimensions, using time-of-arrival information for each click at each hydrophone and the spatial coordinates of the hydrophones (Fig. 2). Distance between source and each hydrophone is computed by methods outlined in Wahlberg *et al.* (2001). The source level at 1 m from the source is calculated for each element of the array, assuming spherical spreading of the sound (see Discussion, Sec. IV) and taking into account frequency-dependent absorption. Since the angular heading of the phonating whale relative to the hydrophone is unknown, the term ASL (apparent source level, see Møhl *et al.*, 2000) is used to emphasize the absence of source heading information.

B. Equipment

Hydrophones were 5 pieces of B&K 8101, 1 piece of Reson 4140, 1 piece of B&K 8105, and 3 pieces of Sonar Products HS150. All hydrophones had a flat (± 2-dB) frequency response in the range from 0.01 to more than 70 kHz. The nominal hydrophone depths were 5, 30, 99, and 327 m. The latter was equipped with a preamplifier, a line driver, and batteries installed in a pressure-resistant canister, connected to the vessel by a steel-armored cable. Calibration was made with B&K 4223 pistonphone calibrators, calibration signals being recorded on every tape at the beginning of each session. The amplifiers were ETEC HA01A, with the high-pass filter set at 0.1 kHz, followed by a two-pole low-pass filter at 11.5 kHz, augmenting the antialias filter of the DAT recorder. The variable level controls of the recorders were clamped in the position of maximum sensitivity, gain being set manually with two-step external attenuators (0 and 40 dB). Recorders were Sony TCD-D3, -D7, -D8, and -D10, sampling at 48 kHz. At one vessel the hydrophone channels were recorded by both DAT recorders and an analog B&K 7606 instrumentation recorder with an upper -6-dB limit at 100 kHz (15 ips), in order to capture possible energy in the sperm whale click above the upper limit (22 kHz) of the DAT recorders.

The positions of the deeper hydrophone were calculated from time-of-arrival measurements by detonators set off at known positions. Sound velocity profiles were obtained with a Star Oddi DST 200 tag, supplemented with hydrographic data from the Institute of Marine Research, Bergen.

C. Analysis

The general approach has been to use the passive sonar equation (Urick, 1983) to derive ASL from received levels, once the position of the whale has been computed from the time-of-arrival differences (TOAD's) *ad modum* Wahlberg *et al.* (2001). The transmission losses (the most influential parameter in the sonar equation) are modeled as spherical spreading plus absorption losses. Sound levels of clicks in the plots below are derived from comparison of the click envelope function with the amplitude of the calibration signal, yielding values in peRMS notation (Møhl *et al.*, 1990). Using this notation, a peRMS measure and a true rms measure of the calibration signal will be identical. With the form factor normally found in sperm whale pulses, a peRMS value of the envelope function is within a few dB of a true rms measure, derived by integration of the waveform over the duration between the -3-dB points of the envelope. True rms values are given for the levels in Table I. The true rms measure is significantly different (yielding lower values) from the peak-to-peak measures, used in most of the literature on odontocete clicks.[2] Energy flux density was calculated using the discrete form of Eq. (11-3) in Au (1993).[3]

For source level estimates, the click had to be identified on more than four platforms, and received level and transmission loss had to be determined. It is a laborious process

TABLE I. Apparent source level, energy flux density, and recording geometry for nine selected clicks of high intensity. Definitions in the text.

Whale ID, time	N[a]	ASL[b] (dB re: 1 μPa rms)	Energy (dB re: 1 μPa^2 s)	Distance whale–hydrophone (m)	Depth (m)	LEP (m)
A 15_135319[c]	5	236±0.5	196	1779	<600	4
B 15_135431[c]	4	234±0.5	193	1369	<400	40
B 15_135519[c]	5	233±0.6	191	1212	<400	14
C 20_163203	5	231±2	189	1431	1005	228
C 20_163503	5	231+2	190	1009	675	226
C 20_163724	5	226±3	186	866	643	224
D 20_204252	4	229+43/−54[d]	186	254	101	13500
E 21_224509	4+2	229±1	188	1135	639	107
E 21_224829	4+1	228±2	187	787	526	107

[a]Number of receivers. Single number indicates shallow (5–30-m depth) hydrophones, and two numbers indicate shallow and deep (100–400-m) hydrophones.
[b]Root-mean-square intensity over duration restricted by −3 dB re: the peak of the click envelope, interpolated with a factor 10 of the sampled data (see Au, 1993). Errors given as 1 s.d.
[c]Array geometry unfavorable for 3D localization. 2D localization is used with depth bounds defined as the seafloor to the surface. These restrictions are incorporated into the calculation of the error in ASL.
[d]Error interval asymmetric due to the logarithmic nature of the transmission loss. The large error for this whale illustrates problems with linear error analysis in certain source-array geometries (cf. Spiesberger and Wahlberg, 2002).

and it is therefore important to select workable click series from the entire material. Accordingly, all tape sequences were scanned manually. Four sets of recordings contained high-level clicks suited for semiautomated click extraction. A property of this approach is that it discards information in the interval between clicks, leaving only some 3% of the original recordings for analysis. Several conditions must be satisfied for automatic click extraction and source location to work, such as good signal-to-noise ratio of the recordings from four or more vessels, absence of other whales and sources of noise, and a suitable geometry between the whale and the set of vessels (Wahlberg *et al.*, 2001). The automated technique was based on a click detector algorithm, which extracted the clicks and aligned them in time. The operator would correct any obvious errors (such as the algorithm detecting the p2 instead of the p1 pulse). Once each click has been timed in the recordings from each vessel, the source position, distance to hydrophones, ASL, etc., can be computed. The purpose of extracting all clicks in a series is that it allows for following signal changes in time and space. The patterns thus obtained are indicative of which parameters are caused by intrinsic properties of the click generator, such as interpulse intervals, and which are consequences of the combination of generator properties with those of the recording geometry, such as directionality and transmission effects. Finally, comparing the development of complete click series at all receivers provides a means for evaluating the consistency of the recordings (e.g., Fig. 3).

III. RESULTS

The main through-going theme of this paper is that the properties of sperm whale clicks differ significantly with as-

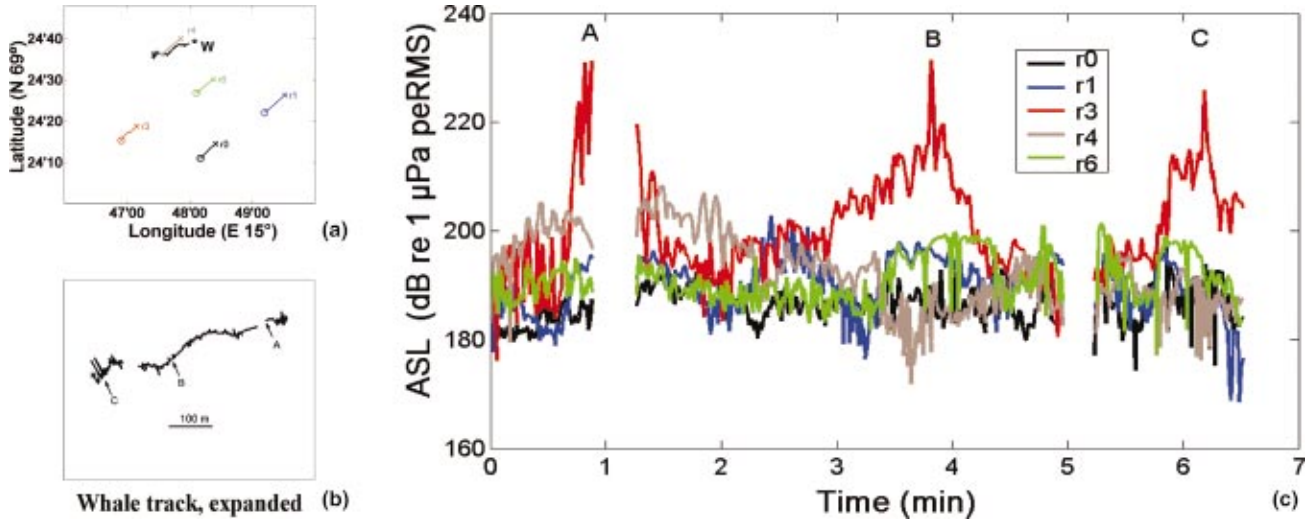

FIG. 3. Acoustic tracking of a sperm whale. (a) Overview of track of whale (westbound surface projected) and array (northeast bound). Hydrophone depths 5–30 m. (b) Whale track expanded. Letters A to C mark whale position during corresponding high-level acoustic events in (c). The small-scale jitter in whale locations is probably caused by uncertainties in the acoustic localization process. (c) ASL for each click at each receiver in the array, using peRMS-notation (see the text).

pect angle. Since direct measures of the heading of the whale are not available, the hydrophone orientation relative to the axis of the animal is in principle unknown. It is assumed that on- and near-on-axis recordings can be distinguished from off-axis recordings by clicks having source levels equal to or above 229 dB *re*: 1 μPa rms. Additionally, on-axis recordings are characterized by p1 pulses being about 40 dB more intense than the remaining pulses of the N&H set, as well as by spectral properties (Sec. III C). This assumption is implicit in the following.

A. Click series

Sperm whale usual clicks are typically emitted in series of tens to hundreds of clicks with a regular or regularly changing repetition rate. A series is defined as limited by silent periods, exceeding the duration of five click intervals in adjacent series (Wahlberg, 2002). Several series may add to form a track. A graphic example of the data from one track with three click series is shown in Fig. 3.

The geometry of recording vessels and whale is given in Fig. 3(a). The vessels are drifting NE with the current, while the whale is moving against the current at a speed through the water of 2 to 3 knots. During the 6 minutes of the track, the whale steadily ascends from a depth of 358 m to 50 m. The detailed, surface-projected 2D track of the whale is in Fig. 3(b), each point of the track representing a position derived from the set of TOADs of a single click at the nodes of the array. The gaps are periods where the whale was silent. The ASL of the click series as seen from the five vessels are plotted in Fig. 3(c), the ordinate given in absolute units, based on calibration, received level, and computed transmission losses. High-level events occur rarely and only at the hydrophone (r3, red) closest to the projected track of the whale. While it would appear that r4 (gray line) in the beginning of the track is on-axis, the r4 levels never get above 210 dB *re*: 1 μPa peRMS. The whale passes this vessel at a depth of some 200 m, and the hydrophone, which is at a depth of 5 m, is likely to be off-axis. The trend of the click rate (not shown) is a small decrease from 1.4 to 1 click/s. The three high-level events in Fig. 3(c) are not accompanied by changes in click rate.

B. Effects of aspect and scan

Directionality of clicks is indicated throughout the recordings by the different appearance of an individual click on the various nodes of the array, as well as in the development over time of a series of clicks, recorded at a single platform. The assumed mechanism for the latter effect is that the whale changes the direction of its sound beam (scanning effect). The difference in waveform of clicks seen from different aspects is illustrated in Fig. 4. The p1 pulse dominates the on-axis signal, and consists of a few cycles (see Fig. 8). The multipulsed pattern is present but not obvious within the dynamic range of a linear plot (Fig. 4, top). In the same click, seen about 20 deg off-axis and amplified (Fig. 4, bottom), the multipulsed pattern is obvious. Notably, the initial event (p0) clearly stands out. The waveform of the off-axis recorded pulses is complicated, consisting of a rather large

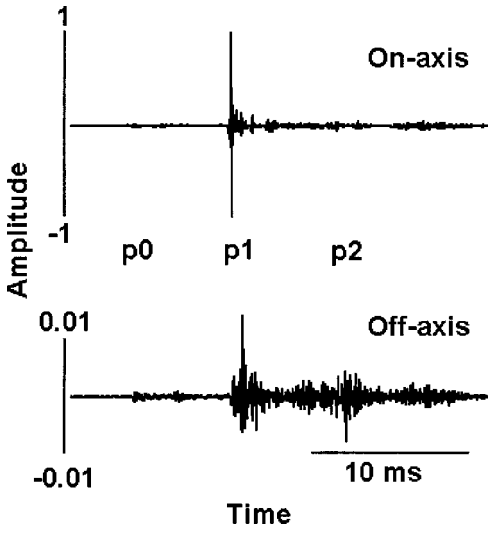

FIG. 4. Same click, recorded at hydrophones r3 (presumably on axis) and r4 (about 20° off axis), obtained 40 s from start of sequence plotted in Fig. 3(c). Gain in lower trace increased by about 40 dB relative to gain in upper trace. The elements of the N&H set are identified.

number of cycles. In between the regularly spaced N&H set considerable click-derived energy occurs, part of which may be surface reflections.

As an example of the scanning effect, the stacked envelopes for a continuous series of 108 clicks, leading up to a presumed on-axis situation, are shown in Fig. 5(a). Note the disproportional increase in p1 intensity towards the end. Also illustrated is the constancy in the timing of the N&H set. In addition to the N&H set, other click-derived pulses occasionally pop up between p1 and p2. In Fig. 5(b), the amplitude of the individual components of the N&H set is given for the same series, relative to a fixed level. It is seen how p1 increases from 12 to about 40 dB above the other pulses, with p2 having a tendency to follow the direction of the changes in p1 amplitude. The p0 amplitude is changing rather little.

Looking at the evolution of the spectra of the p1 pulse of this click series (Fig. 6), it is seen how the spectra of the off-axis clicks before the end of the series have many peaks and notches. The spectra of near-on-axis clicks at the end of the series are smooth, with a broadband appearance and with the frequency of maximum energy shifted upwards.

C. On-axis p1 pulse properties

In on-axis clicks as defined above, only p1 of the N&H set is seen in the waveform displays (Figs. 4, top 7a). The large dynamic range of the envelope function in decibel format reveals the rest of the set, at levels about 40 dB below the p1 pulse (Fig. 7b).

When energy flux density is calculated over the 25-ms time function of the click in Fig. 7(a), 99.6% of the energy is found in the p1 pulse. Energy flux densities for a collection of clicks are given in Table I. For comparison, energy flux densities of clicks from four species of dolphins are lower by 30 to 80 dB (Au, 1993, Table 7.3).

The p1 pulse of an on-axis signal (Fig. 8) has a simple waveform, dominated by a single cycle. The duration of the

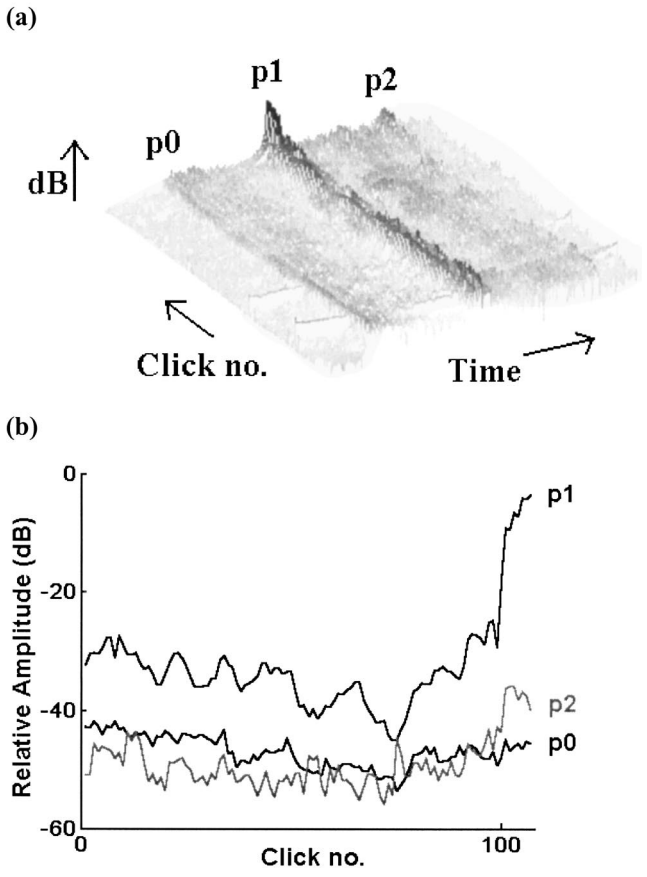

FIG. 5. A series of 108 consecutive sperm whale clicks from a series lasting $1\frac{1}{2}$ min and progressing from an off- to an on-axis condition (last 6 clicks). The whale is approaching from a distance of 1 km and a depth of 0.8 km. Hydrophone depth: 30 m. (a) (waterfall format) shows the log of the envelope functions in 20 ms around each click, aligned by the p1 peak. In (b), the elements of the N&H set for each click have been extracted and the relative amplitude plotted.

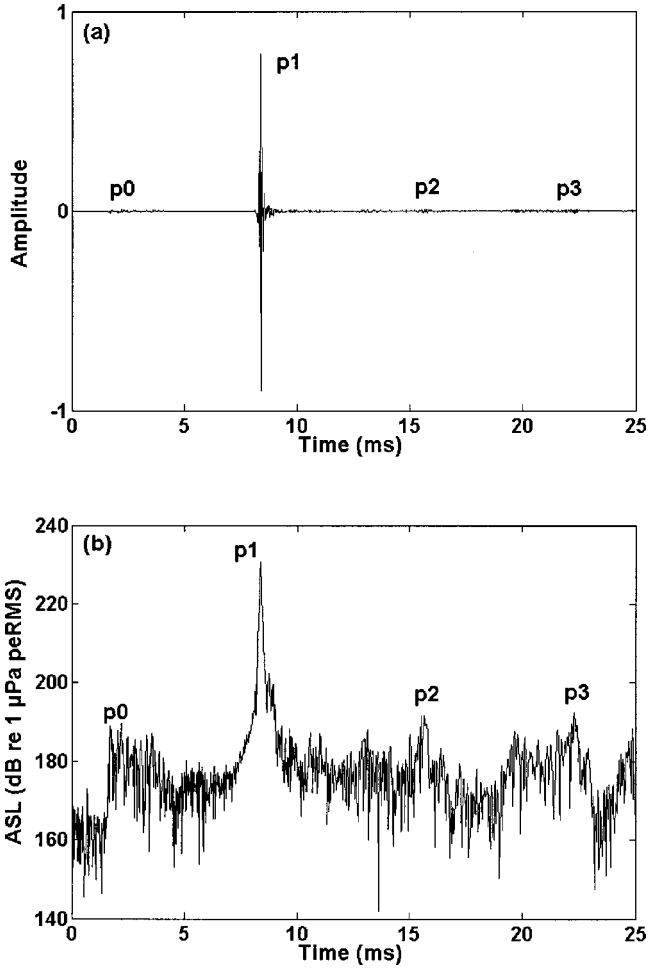

FIG. 7. Time series of an on-axis click (a) in oscillogram format; (b) in *log(envelope)* format. Distance between the whale and the hydrophone is about 1 km.

p1 pulse at the −3-dB limits on the envelope function is 52 μs, 114 μs at the −10-dB limit (Fig. 8).

The Woodward time resolution constant (Au, 1993), defining the theoretical range resolution of a signal for sonar purposes, is 71 μs for the p1 pulse in Fig. 8, corresponding to a range uncertainty of about 11 cm. The product of the time resolution constant and the centralized rms bandwidth (cBWrms; Au, 1993) is 0.29, numerically similar to what is found in *Tursiops* (data from Au, 1993, Table 10.1).

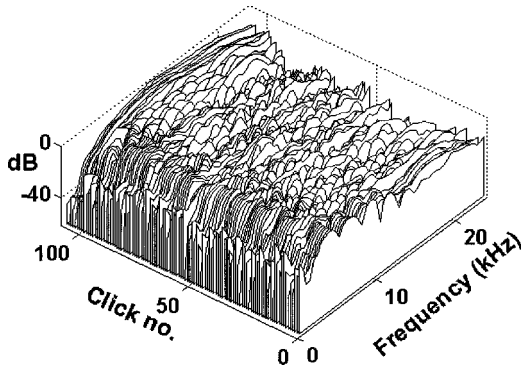

FIG. 6. Spectra of the p1 pulses in the series shown in Fig. 5. Bin width of FFT: 375 Hz; Hanning window.

The spectra of the set of N&H-pulses of this on-axis click are presented in Fig. 9. The p1 spectrum is smooth, peaking around 12 kHz, while the spectra of p2 and p0 have many peaks and notches, possibly indicating a multipath history. As numerical measures of the spectral properties, the centroid frequency (the frequency splitting the spectrum den-

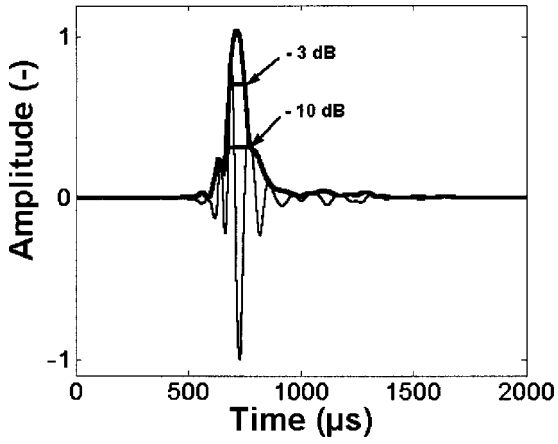

FIG. 8. Waveform and envelope of an on-axis p1 pulse. The −3- and −10-dB limits are added.

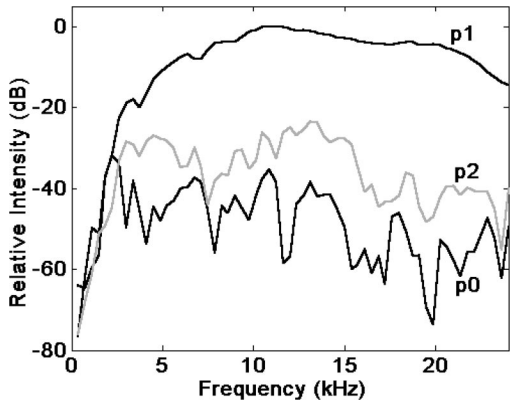

FIG. 9. Spectra of the N&H set of the on-axis click in Fig. 7(a). Bin width of FFT: 375 Hz; Hanning weighting employed.

sity into two equally sized halves; Au, 1993) and the centralized rms bandwidth are given in Table II.

Analysis of on-axis data recorded with the instrumentation recorder shows that the p1 spectrum extends with decreasing magnitude to 40 kHz, above which the signal is masked from noise in the analog recording process.

D. Intensity of on-axis p1

As evidenced by Fig. 3, on-axis events, as defined above, are rare. The maximum SL for any click in our recordings is 236 dB *re*: 1 μPa rms (Table I), with eight other independent events in the range from 226 to 234 dB. In Table I, only the most intense click of a given series is listed. In seven of these events, the whale is on the ascending leg of the dive, with the hydrophones closer to the surface. The general heading of the whales during such events is towards the one hydrophone registering the presumed on-axis event, except in one case, where the hydrophone is rather abeam of the whale's heading. It is noted that the sampling frequency of the position of the whale is dictated by the click rate and probably not coupled to the movements of the whale in a way satisfying the sampling theorem. At the moment of click transmission, the whale may thus point in a direction that is different from the one given by the line between neighboring fixes. For the discussion below, 235 dB *re*: 1 μPa rms is chosen to be representative for the on-axis SL.

In summary, an on-axis click is characterized by its high source level and additionally by having almost all energy contained in the p1 pulse. The spectrum of the p1 pulse has more energy at high frequencies than have off-axis p1 pulses. The waveform and time–bandwidth product of the p1 pulse is similar to that of on-axis clicks from bottlenose dolphins, but the centroid frequency is lower by an order of magnitude.

TABLE II. Spectral properties of N&H pulses of the on-axis click in Fig. 7(a). Definitions in text.

Pulse no.	Centroid frequency (kHz)	cBWrms (kHz)
p0	7.2	5.0
p1	13.4	4.1
p2	10.7	4.2
p3	12.1	3.5

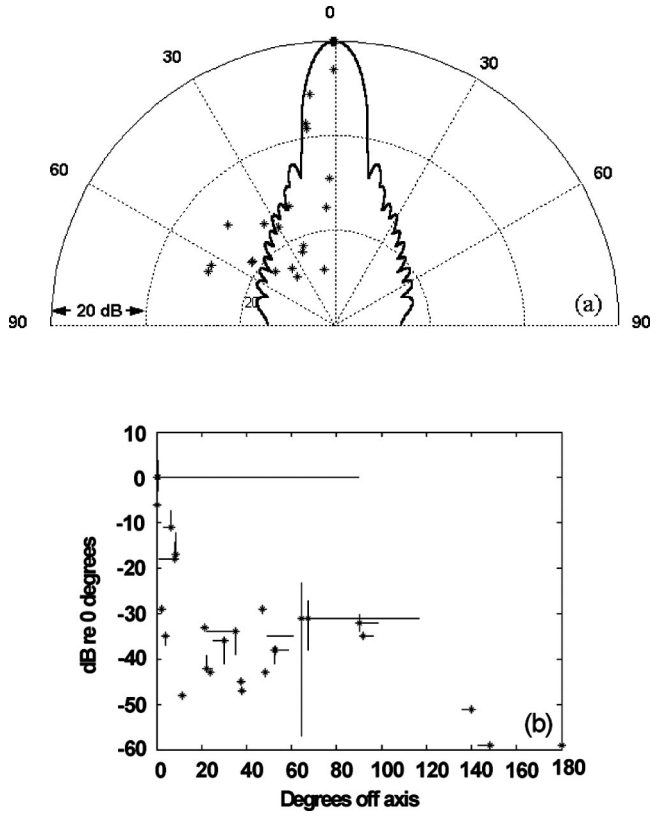

FIG. 10. Composite directionality pattern, based on 6 clicks with on-axis properties recorded by one hydrophone of the array. The radiation pattern is assumed to be rotationally symmetric around the axis of the animal. The dots are plotted as the difference in level and angle from the on-axis recording to recordings from other hydrophones for each click (see Fig. 2 for an example of the recording situation). In (a), the thick line is the theoretical radiation pattern of a circular, 80 cm diameter piston in a baffle, transmitting a p1 pulse as in Fig. 8. (b). 95% error bars, obtained from linear error propagation analysis (see text).

E. Directionality

Since specific information about whereto the whale is directing its beam of sound is unobtainable with the methods used, a radiation pattern in the conventional sense (Au, 1993) cannot be constructed. However, if we assume that a click seen from a hydrophone with ASL$\geqslant$229 dB is on-axis relative to that hydrophone, the aspect angle for each of the other hydrophones can be calculated. If we furthermore assume that the radiation pattern is rotationally symmetric around the acoustic axis, a radiation pattern can be obtained (Fig. 10).

The points plotted in Fig. 10(a) are the data from six clicks in Table I with an ASL of 229 dB or larger (whale D in Table I is excluded due to the large location error). The directional pattern predicted from a plane piston with a diameter of 80 cm (the estimated size of the flat, frontal surface of the junk) emitting the on-axis pulse of Fig. 8, is shown bilaterally (fat line). The half power, half-angle of this function is 4°, and the directional index (DI) is 27 dB.

To illustrate the uncertainties caused by the localization process as determined by linear error propagation analysis (LEP, Wahlberg *et al.*, 2001), the data have been replotted in

Fig. 10(b) with error bars for source level and angle added for each point. The large angular error on axis is caused by a single click (whale B in Table I), where the geometry was unfavorable for localization.

The DI may also be calculated directly from the data set, using the discrete version of Eq. (3.10) in Au (1993)

$$\mathrm{DI} = 10 \log_{10} \frac{2}{\sum_{i=1}^{N} b_i \sin \nu_i \Delta \nu}.$$

In this equation, b_i is the ith sample of an interpolation of the discrete beam pattern; ν is the angle to the acoustic axis; and $\Delta\nu$ is the angular increment between the ith and $i+1$th sample of ν. N is the number of samples, and ν is running from 0 to π radians. This formula assumes that the beam pattern b is rotationally symmetric around the acoustic axis. With the data in Fig. 10(a), the directional index of sperm whale clicks is calculated to be 27 dB, identical to the value derived from the piston model above. However, the precision of this estimate is unknown, due to the variation in the precision of the primary data illustrated in Fig. 10(b).

IV. DISCUSSION

A. Sources of error

The results presented above differ markedly from the classical descriptions of sperm whale clicks (Backus and Schevill, 1966; Levenson, 1974; Watkins, 1980). This is true for the click structure and directionality, as well as for the maximum SL. Differences of 50 to 60 dB in the maximum SL are noteworthy. The results are qualitatively in line with those of three other, large-aperture array recordings (Whitney, 1968; Møhl *et al.*, 2000; Thode *et al.*, 2002). The quantitative differences from the previous large-aperture results are likely a consequence of the low probability of having a single hydrophone in the narrow beam of the whale, combined with differences between the arrays in number of hydrophones, virtual as well as real [surface and bottom reflected signals as used by Thode *et al.* (2002) can be treated as records from virtual hydrophones, mirrored by the surface or the bottom]. The absolute SLs found are significantly higher than the levels reported from any sound-producing species. Since the findings presented are obtained with a novel technique, it will first be discussed if some kind of error could account for such findings.

1. Trivial errors

Trivial errors are for example calibration errors. Equipment and operator malfunctions in the running of a complex setup cannot be totally eliminated, but they can be minimized. The procedure of recording a pistonphone calibrator signal on the tapes of each session, and keeping the digital tape log information about recording conditions inseparable from the sound track, helped to keep trivial errors from proliferating. Redundancy in vessels and hydrophones allowed for omission of the occasional recording that for one reason or another was not acceptable, without falling short of the requirements for acoustic localization. The consistency of the data in Fig. 3, and indeed throughout the data set, is evidence that trivial errors were not common. No recording from any single vessel exhibits a constant bias in received sound level.

2. Localization errors

Errors of a different kind are found in the limited precision of localization. An error in the estimated range between the whale and the hydrophone translates into an error in the estimated ASL. As seen from Table I, column 3, such effects can be quite large, but not large enough to distort the general picture of a number of clicks with ASLs above 230 dB *re*: 1 μPa rms. The localization uncertainty depends on the geometry of the source and the receivers. It is not constant, and therefore it is difficult to apply uncertainty to the DI estimates. The LEP values in Table I and Fig. 10(b) give the composite localization uncertainty for particular clicks. It varies from a few whale lengths to 13.5 km. The LEP values are dominated by uncertainty in the determination of whale depth, a consequence of the majority of the hydrophones being only 5 to 30 m below the surface. Figure 3(b) shows that the click-to-click positional scatter is smaller than the LEP derived uncertainty by about 1 order of magnitude. This is largely explained by the omission of depth information in the 2D plot of Fig. 3(b), as well as by methodological problems with the LEP technique in some source-array geometries (Spiesberger and Wahlberg, 2002).

3. Transmission anomalies

Transmission anomalies have a potential for invalidating the model of spherical spreading. Transmission loss compensation is by far the largest parameter entering the computation of source levels. The sound velocity profile is a fairly simple one (see Sec. II). Ray tracings show some ray bending to be present, resulting in shadow zones for distant whales near the surface, and also creating conditions for caustics (Medwin and Clay, 1998). Such ray bending can change the levels of the received clicks considerably, and may raise questions about the validity of the extreme source levels listed in Table I.

However, the data on relative amplitude changes of the N&H set leading up to a presumed on-axis event should be noted. The rate of increase in levels associated with p1 is neither seen in the other pulses (Fig. 5), nor in off-axis recordings of p1 (Fig. 3c). Any transmission anomaly, such as caustics, would operate equally on all pulses of a set. Another observation is the flattening and expansion of the spectrum towards higher frequencies near on-axis (Fig. 6; also indicated in Møhl *et al.*, 2000, Fig. 7). Caustics will not change the spectral properties of a pulse, only amplitude and phase (Medwin and Clay, 1998). We consequently dismiss caustics as a likely mechanism behind the pattern in Fig. 3(c) and the high levels in Table I. Some other possible effects, such as constructive interference caused by multipath interactions, can be dismissed from the same line of reasoning.

B. Directionality

The combined observations of 1, scarcity of on-axis clicks, 2, their extreme intensity, 3, that high-level clicks are prevailingly recorded in the general course of the whale and

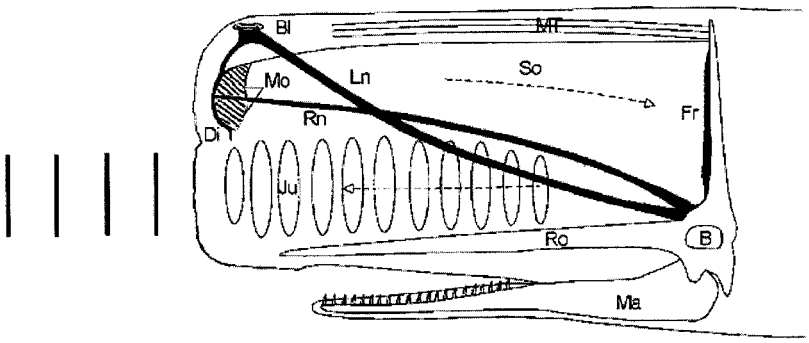

FIG. 11. Diagram of anatomical structures in the sperm whale nose. **B**, brain; **Bl**, blow hole; **Di**, distal air sac; **Fr**, frontal air sac; **Ju**, junk; **Ln**, left naris; **Ma**, mandible; **Mo**, monkey lips; **MT**, muscle-tendon layer; **Ro**, rostrum; **Rn**, right naris; **So**, spermaceti organ. Spermaceti oil is contained in the spermaceti organ and in the spermaceti bodies of the junk. Arrows indicate the assumed sound path from the generating site (**Mo**) back to the reflecting frontal sac (**Fr**) and forward and out through the junk (**Ju**). Sound waves of low divergence are symbolically indicated in front of the whale. (Modified from Madsen *et al.*, 2002a.)

during its ascent (most hydrophones were shallow ones), and 4, that high-level clicks are only recorded by one hydrophone at a time in the set of five or more hydrophones, may all be explained by the high directionality of the clicks. It is emphasized that while Fig. 10 is believed to be the first directionality pattern obtained from any odontocete species in an open ocean environment, it is obtained by a nonstandard method and based on a number of assumptions. The fact that it has been achieved at all was unexpected, since the array was designed to obtain data on source levels, not on directionality.

As the angles between the whale, the ''highlighted'' hydrophone, and the other hydrophones are not controllable, favorable geometries are rare in the material. Particularly, several hydrophones at small angles relative to the highlight direction tend to generate hyperboloid surfaces in the localization calculations that are almost parallel to each other, thereby increasing the positional uncertainty. Another reservation concerns the composite origin of the data, derived from clicks from different whales and recording geometries, and the classification of clicks above or equal to 229 dB *re*: 1 μPa rms as being on-axis clicks. It is consequently not possible to compute a directional index with a meaningful measure of accuracy. Still, the results in Fig. 10 are internally consistent, indicating a half-angle, half-power beam width of about 4°, comparable to that of *Tursiops* (Au, 1993, Table 6.1). Thus, the use by the sperm whale of wavelengths one order of magnitude larger than those of the dolphin is compensated for by other means, of which size is an important factor.

Au *et al.* (1986) show that the radiation pattern of dolphins can reasonably be modeled by radiation from a flat, circular piston with a diameter of 8 cm. Piston modeling of the sperm whale generator is particularly appealing, since the frontal surface of the junk can indeed be flat (Møhl, 2001, Fig. 3) and about 80 cm in diameter in adult males as found off Andenes. Accepting that the supracranial structures of the sperm whale are the generator of sound, and that sound exits the system at the front of the junk (Møhl and Thiele, 1981; Cranford, 1999; Møhl, 2001; Møhl *et al.*, 2003), an increase in aperture relative to that of the dolphin of the same order of magnitude as the increase in wavelength thus seems to be realized. The radiation pattern of the piston model applied to the sperm whale is given in Fig. 10(a). It is seen that this function is generally wider than the function generated by the data points up to about 50 degrees. No mechanism has been identified that could bias the measurements towards smaller, angular estimates. Therefore, it is suggested that the sperm whale's sound-transmitting mechanism could be more sophisticated than what may readily be explained by the theory of the plane piston. This observation may support the bent-horn model (Møhl, 2001; Møhl *et al.*, 2003) that sees the spermaceti organ and junk compartment as two connected tubes, forming a bent, conical horn.

The bend is at the frontal sac (Fig. 11), directing sound generated at the monkey lips (Madsen *et al.*, 2003) from the spermaceti compartment into the junk. A conspicuous feature of the latter is the wafer-like bodies of spermaceti, often referred to as lenses, regularly spaced along the distal part of the junk. It is speculated that these wafers may have a function of adjusting the phase of the p1 pulse over the entire cross section of the horn, producing a flat wavefront at the exit surface. The combined length of this horn is twice the length of the spermaceti organ, or about 10 m in an adult male, and the assumed aperture (the frontal, flat termination of the junk) is about 0.8 m as mentioned above. It is proposed that the function of this horn, as well as the evolutionary drive behind its formation, is the generation of the on-axis, narrow-beam, monopulsed click.

It follows from the procedure for generating the composite radiation pattern presented in Fig. 10 that clicks with ASLs lower than 229 dB *re*: 1 μPa rms will not enter the computation. A consequence of this is that if the whale has control over the width of the beam and an ability to trade SL for beamwidth, such effects will not show up in the data. The same will happen if the whale turns down click amplitude. Control of click amplitude has recently been reported from an experiment with a suction cup fixated hydrophone on a diving sperm whale (Madsen *et al.*, 2002a). Fine control of the anatomical structures in the nasal complex is indicated by the observation by Oelschläger and Kemp (1998) that the trigeminal and facial nerves innervating the nasal musculature in the sperm whale, have three to eight times the count of fibers found in other odontocetes. The muscles and tendons associated with the spermaceti complex are massive and subdivided into small bundles as thick as a finger in adult specimens. Thus, from an anatomical viewpoint it seems likely that the shape of the spermaceti complex can be changed, possibly controlling the beam pattern. However, the whale also requires controlling elements to adjust the type of clicks, their repetition rate and amplitude (Madsen *et al.*, 2002a); hence, the mere presence of controlling nerves and muscles is not exclusively suggestive of a beamforming mechanism.

C. The acoustic properties of the on-axis p1 pulse

Only about one in a thousand clicks recorded was of the on-axis, monopulsed type (Fig. 7a). Thus, the likelihood of recording such clicks with conventional, single hydrophone methods (Backus and Schevill, 1966; Levenson, 1974; Weilgart and Whitehead, 1988; Gordon, 1987) or small aperture arrays (Watkins and Schevill, 1977) is lower than for large-aperture arrays. Another important factor is the often-used strategy of approaching the whales when surfaced and starting the recordings after fluking. This strategy allows for photo identification of the whale, but also increases the likelihood of off-axis recordings, as pointed out by Goold and Jones (1995). In addition to the unfavorable statistics for on-axis recordings, there is the problem of their extreme intensity, requiring a large dynamic range in the recording chain, if the much more abundant off-axis clicks and the N&H set of on-axis clicks are also to be properly recorded. And, the off-axis clicks must be recorded, both for IPI and ICI (interclick interval) determinations, and for TOAD determinations. Our earlier recordings of this species (Møhl and Amundin, 1991; Møhl *et al.*, 2000) had putative on-axis clicks distorted, thus excluding estimation of true ASLs.

All these technicalities add up to an explanation why the classical picture of sperm whale usual clicks is that of multipulsed, low-intensity, nondirectional sounds. The present data suggest that this picture is based on sound energy recorded off the main beam and, therefore, of no relevance to the echolocation capabilities of the species. Realizing that 99.6% of the energy is contained in the p1 pulse, the click is essentially single pulsed, as is the illumination of sonar targets on which the whale may train its beam.

The intensity of a sound with a source level of 235 dB *re*: 1 μPa rms may not readily be appreciated outside the community of underwater acousticians. This is the most intense sound recorded from any animal. Converted to sound pressure of a similar intensity in air, the level corresponds to 173 dB SPL (*re*: 20 μPa). The intensity is 10–14 dB above what can be measured 1 m in front of the muzzle of a powerful rifle. The peak power required for generating an omnidirectional pulse in water with a source level of 235 dB *re*: 1 μPa (rms) is 2 MW (at a conversion efficiency of 100%). Accepting a DI of 27 dB reduces this number to 4 kW, which is still a truly remarkable sound power value, possibly indicating the DI to be underestimated. The megawatt value is given here only to illustrate the consequences if the concept of low or no directionality in sperm whale usual clicks (Watkins, 1980) is applied to the SLs reported in this paper.

The duration of the p1 pulse as measured at the -10-dB limits of the envelope function is about 100 μs. This is slightly longer than the 50–80 μs given for bottlenose dolphins, but in the low end of the range of 50–400 μs for 41 odontocete species (Au, 1993, Table 7.2). Another property of the p1 on-axis pulse shared with echolocation clicks of dolphins (Au, 1980) is the broadening and flattening of the spectrum on-axis relative to off-axis recordings, as shown in Fig. 6. The spectral peaks and notches seen in the off-axis clicks of Fig. 6 are also observed in off-axis recordings of dolphins, were they may be explained by multipath transmission inside the sound production organ (Au, 1993).

D. Sonar properties of the on-axis p1 pulse

Since the monopulsed sperm whale click has properties that are particularly well suited for long-range sonar, this section will explore this putative sonar function. It is recognized that a formal proof of the use of biosonar in any free-ranging species is hard to obtain. This fact should be kept in mind, but not prevent the analysis from being made.

Sonars can be evaluated from the set of sonar equations (Urick, 1983). Using an elaborate form of the sonar equation (the transient form), predictions on dolphin sonar and actual measurements of performance agree quite closely (Au and Penner, 1981; Kastelein *et al.*, 2000). However, the basic sonar equation for the noise-limited case, using intensity terms on dB form, is instructive for illustrating the significance and interaction of the parameters. Specifying the source level (SL), transmission loss (TL, $40 \log r + r\alpha$, α being absorbtion), noise level (N), receiver directionality (DI), and target strength (TS), the detectability (DT) of a given target and range can be predicted (Urick, 1983)

$$\mathrm{DT} = \mathrm{SL} - 2\mathrm{TL} + \mathrm{TS} - \mathrm{NL} + \mathrm{DI}.$$

Using a target strength of a single squid (*Loligo*) of -40 dB (Schmidt, 1954), a transmission loss consisting of the two-way spreading loss plus an absorption of 1.5 dB/km, an SL of 235 dB *re*: 1 μPa, a spectrum level of background noise at sea state 1 of 35 dB *re*: 1 μPa applied over the cBWrms of 4.1 kHz of the p1 pulse around its centroid frequency, and finally assuming a directionality of the ear like that of dolphins (21 dB at 120 kHz; Au and Moore, 1984), a DT for this *Loligo* will be in the order of 20 dB at a range of 1 km. The main factor behind this remarkable DT at such a long range is the source level. The choice of masking bandwidth of the noise has minor effects but does include a hypothesis about the detector (Menne and Hackbart, 1986). Here, an energy detector is assumed. It is noted that the absorption term has a minimal impact due to the relatively low frequencies of the pulse spectrum. If instead a pulse with the spectrum of that of a dolphin (100 kHz) were used *ceteris paribus*, the detectability would be reduced by about 60 dB by absorption at this range.

Another conclusion from applying the noise-limited form of the sonar equation is that noise is unlikely to be the primary limitation of the putative sonar. Instead, clutter or reverberation caused by reflectors other than the target is a likely limiter. Effects of clutter are reduced with increased directionality. The narrow beam suggested by the data in Fig. 10 might be seen in this light. No information about the hearing directionality of sperm whales has been reported.

The classical scatter function of reflection versus wavelength divided by target cross section (Urick, 1983) show a diminishing return for targets with radii of less than 3 cm for p1 pulse signals. Sperm whales are remarkable for eating prey of all sizes from sardines to sharks several meters long (Berzin, 1972). Echoes from the p1 pulses could in theory be reflected from a single sardine without excessive attenuation by entering the Rayleigh scattering region.

Dolphins scan their surroundings with their sonar beam, using click rates on the order of 100 pulses per second. Since the clicking rate of sperm whales for the kind of clicks dealt

with here is in the order of 1 pulse per second, while the directionality of the clicks may be as high as that of dolphins, it follows that the acoustic images of the surroundings obtainable by these two types of biosonar must be quite different (that of the sperm whale being more patchy). However, as pointed out by Dubrovsky (2001, personal communication), a possible analogy might be to vision, where foveal vision is only covering a few degrees, with extrafoveal vision adding coarse information to the general picture. Thus, the low-level sidelobes in Fig. 10 may still convey information to the whale from nearby objects or from objects with high target strengths, although not as detailed as that from the main beam. Based on such ''extrafoveal'' information, the whale might choose to train its narrow beam towards targets of potential interest. Another possibility, which cannot be examined with the present data, is that the directional pattern may not be fixed but controlled by the whale, adapting DI to the detection task at hand. Finally, click series with high repetition rates called creaks have been reported (Weilgart and Whitehead, 1988; Gordon, 1987), and tentatively ascribed a function similar to buzzes from echolocating bats (Madsen *et al.*, 2002b).

In summary, the properties of the on-axis p1 pulse: the high-SL values, low absorption, high directionality, low time-bandwidth product, and geometric backscatter properties for target with radii down to 3 cm are seen individually and combined to be adaptations for maximizing sonar range for prey detection. The slow click rate indicates long range, but also that the angular sampling of the surroundings must be limited. The findings presented here lead to conclusions about the sonar properties of the sperm whale click that are at odds with conclusions of previous work. Since the discrepancies are rooted in the properties of the p1 pulse as described *de novo* here, comparisons to previous assessments are not meaningful.

E. The monopulse click and its relation to the Norris and Harvey theory

The interpretation of the N&H set (Fig. 1) is that the p0 pulse signals the primary event at the monkey lips, transmitted as a leakage directly to the medium. The interval between onset of this pulse and p1 is reportedly less than that of the remaining pulses of the set (Møhl and Amundin, 1991). The main pulse is p1, being shaped by traveling through the spermaceti and junk compartments once. The remaining pulses are stray energy from the p1 pulse, making the two-way travel inside the nasal structures an additional number of times. The view presented above on the intrinsic monopulsed nature of the sperm whale on-axis click and its implications for the way the sound generator works (the bent-horn model) should not be perceived as an alternative to the Norris and Harvey model, but rather as an extension of it. The original Norris and Harvey (1972) model for sound generation in the sperm whale has been successful in explaining the mechanism behind the interpulse intervals. The bent-horn model is a descendant of the Norris and Harvey model, incorporating evidence not available when the original model was formed. Such evidence is (1) the observation of p0 as an indicator of the primary sound generation event (Møhl and Amundin, 1991), (2) the observation that the pulses (except for p0) tend to be in phase with each other (Møhl and Amundin, 1991), as opposed to having even-numbered pulses being phase reversed relative to uneven-numbered pulses as in the analog model constructed by Norris and Harvey; (3) the inferred addition of the junk to the pathway of the sound (Møhl and Thiele, 1981; Cranford, 1999); (4) extreme source levels and high directionality of the clicks (Møhl *et al.*, 2000; Thode *et al.*, 2002; this paper), and (5) the monopulsed nature of the on-axis click. Observation 2 suggests that p0, being the ancestor to the rest of the N&H set, is largely contained in the system. Only a tiny fraction [see Fig. 7(b)] is leaking out directly from the source (the monkey lips; Madsen *et al.*, 2003) to the medium, the distal sac possibly acting as a sound screen. The bulk of the energy is traveling rearwards towards the frontal sac, where it is reflected and directed forward through the junk, exiting as p1 (see Fig. 1). The p2 pulse, again of insignificant amplitude, is proposed to be a fraction of the p1 pulse that does not get into the junk but is returned to the spermaceti organ, then being reflected a second time at the distal sac and subsequently a third time by the frontal sac. Each reflection introduces a phase shift of 180 deg. The higher numbered pulses are repeats of the history of p2. According to this scheme, p1 is phase reversed once, p2 three times, p3 five times. Thus, all pulses will appear as having the same phase. It should be emphasized that this relationship is not seen in all clicks.

The off-axis click properties known to Norris and Harvey were quantitatively quite different from the on-axis properties, likely to be those that matter to the sperm whale. Still, Norris and Harvey came up with a model containing all the essential mechanisms behind click generation in the sperm whale. It is remarkable that their modeling was in fact facilitated by what would now appear to be off-axis signals.

V. CONCLUSIONS

The bent-horn model adds to the collection of quite divergent ideas on the functional anatomy and evolutionary drive behind the development of the nasal complex in sperm whales. Other proposals are: a hydrostatic organ (Clarke, 1970), the single tube, multipulse sound generator (Norris and Harvey, 1972), a nitrogen sink (Schenkkan and Purves, 1973), a device signaling sexual qualities (Gordon, in Goold and Jones, 1995; Cranford, 1999), and a ramming device in male–male fighting (Carrier *et al.*, 2002). While the bent-horn model is based on the Norris and Harvey scheme, it goes further by linking the extraordinary anatomical proportions and complexity of the sperm whale head with the equally extraordinary acoustic properties of the monopulsed click.

ACKNOWLEDGMENTS

We thank the crews, skippers, and owners of MALLEMUKKEN, SIGNE RINK, IOLAIRE, and R/V NARHVALEN for providing the ''backbone'' of the array. We also thank recordists M. F. Christoffersen, O. Damsgaard, L. A. Miller, B. K. Nielsen, M. H. Rasmussen, M. Simon, A. Surlykke, J.

Tougaard, and F. Ugarte. N. U. Kristiansen developed and assembled the electronics. Andenes Whale Safari and Svein Spjelkavik, Hisnakul, Andenes, provided shore base facilities and support. The Danish Research Council, through The Center for Sound Communication, SDU, funded this work.

[1]Several types of sperm whale clicks can be distinguished (Gordon, 1987; Weilgart and Whitehead, 1988). The most abundant type, and the one, with which this paper deals, is called ''usual clicks.'' Additional types are discussed in Madsen *et al.* (2002b).

[2]Au (1993, p. 130) states the pp measure of a *Tursiops* click is 15.5 dB above the true rms measure.

[3]$E=(1/\rho c)\Sigma_i p_i^2 \Delta t$, where ρ is the density, c is the sound velocity, p_i is the ith sample of the sound pressure, and Δt is the sample interval.

Au, W. W. L. (**1980**). ''Echolocation signals of the Atlantic bottlenose dolphin (*Tursiops truncates*) in open waters,'' in *Animal Sonar Systems*, edited by R. G. Busnel and J. F. Fish (Plenum, New York), pp. 251–282.

Au, W. W. L. (**1993**). *The Sonar of Dolphins* (Springer, New York).

Au, W. W. L., and Penner, R. H. (**1981**). ''Target detection in noise by echolocating Atlantic bottlenose dolphins,'' J. Acoust. Soc. Am. **70**, 251–282.

Au, W. W. L., and Moore, P. W. L. (**1984**). ''Receiving beam patterns and directivity indices of the Atlantic bottlenose dolphin, *Tursiops truncatus*,'' J. Acoust. Soc. Am. **75**, 255–262.

Au, W. W., Moore, P. W., and Pawloski, D. (**1986**). ''Echolocation transmitting beam of the Atlantic bottlenose dolphin,'' J. Acoust. Soc. Am. **80**, 688–691.

Backus, R. H., and Schevill, W. E. (**1966**). ''Physeter clicks,'' in *Whales, Dolphins, and Porpoises*, edited by K. S. Norris (University of California Press, Berkeley), pp. 510–528.

Berzin, A. A. (**1972**). *The Sperm Whale* (Israel Program for Scientific Translations, Jerusalem).

Carrier, D. R., Debahn, S. M., and Otterstrom, J. (**2002**). ''The face that sunk the Essex: Potential function of the spermaceti organ in aggression,'' J. Exp. Biol. **205**, 1755–1763.

Ciano, J. N., and Huerle, R. (**2001**). ''Photo-identification of sperm whales at Bleik Canyon, Norway,'' Marine Mammal Sci. **17**(1), 175–180.

Clarke, M. R. (**1970**). ''Function of the spermaceti organ of the sperm whale,'' Nature (London) **228**, 873–874.

Cranford, T. W. (**1999**). ''The sperm whale's nose: Sexual selection on a grand scale?'' Marine Mammal Sci. **15**, 1133–1157.

Cranford, T. W., Amundin, M., and Norris, K. S. (**1996**). ''Functional morphology and homology in the odontocete nasal complex: Implications for sound generation,'' J. Morphol. **228**, 223–285.

Dubrovsky, N. (**2001**). Personal communication.

Dunn, J. L. (**1969**). ''Airborne measurements of the characteristics of a sperm whale,'' J. Acoust. Soc. Am. **46**, 1052–1054.

Fristrup, K. M., and Harbison, G. R. (**2002**). ''How do sperm whales catch squids?'' Marine Mammal Sci. **18(1)**, 42–54.

Goold, J. C., and Jones, S. E. (**1995**). ''Time and frequency domain characteristics of sperm whale clicks,'' J. Acoust. Soc. Am. **98**, 1279–1291.

Gordon, J. C. (**1987**). ''The behaviour and ecology of sperm whales off Sri Lanka,'' Ph.D. thesis, University of Cambridge.

Gordon, J. C. (**1991**). ''Evaluation of a method for determining the length of sperm whales (*Physeter catodon*) from their vocalizations,'' J. Zool. **224**, 301–314.

Kastelein, R. A., Au, W. W., and de Haan, D. (**2000**). ''Detection distances of bottom-set gillnets by harbor porpoises (*Phocoena phocoena*) and bottlenose dolphins (*Tursiops truncatus*),'' Mar. Environ. Res. **49**, 359–375.

Levenson, C. (**1974**). ''Source level and bistatic target strength of the sperm whale (*Physeter catodon*) measured from an oceanographic aircraft,'' J. Acoust. Soc. Am. **55**(5), 1100–1103.

Madsen, P. T., and Møhl, B. (**2000**). ''Sperm whales (*Physeter catodon* L.) do not react to sounds from detonators,'' J. Acoust. Soc. Am. **107**, 668–671.

Madsen, P. T., Payne, R., Kristiansen, N. U., Wahlberg, M., Kerr, I., and Møhl, B. (**2002a**). ''Sperm whale sound production studied with ultrasound time/depth-recording tags,'' J. Exp. Biol. **205**, 1899–1906.

Madsen, P. T., Wahlberg, M., and Møhl, B. (**2002b**). ''Male sperm whale (*Physeter catodon*) acoustics in polar waters: Implications for echolocation and communication,'' Behav. Ecol. Sociobiol. **53**, 31–41.

Madsen, P. T., Carder, D. A., Au, W. W. L., Møhl, B., Nachtigall, P. E., and Ridgway, S. H. (**2003**). ''Sound production in neonate sperm whales,'' J. Acoust. Soc. Am. **113**(6), 2988–2991.

Medwin, H., and Clay, C. C. (**1998**). *Fundamentals of Acoustical Oceanography* (Academic, New York).

Menne, D., and Hackbarth, H. (**1986**). ''Accuracy of distance measurement in the bat *Eptesicus fuscus*: Theoretical aspects and computer simulations,'' J. Acoust. Soc. Am. **79**, 386–397.

Møhl, B. (**2001**). ''Sound transmission in the nose of the sperm whale, *Physter catodon*. A *post mortem* study,'' J. Comp. Physiol., A **187**, 335–340.

Møhl, B., and Amundin, M. (**1991**). ''Sperm whale clicks: Pulse interval in clicks from a 21-m specimen,'' in *Sound Production in Odontocetes, with Emphasis on the Harbour Porpoise, Phocoena phocoena*, edited by M. Amundin (Stockholm).

Møhl, B., and Thiele, L. (**1981**). ''Hvaler og støj i havet (Whales and underwater noise),'' Fisk og Hav **39**, 49–55.

Møhl, B., Surlykke, A., and Miller, L. A. (**1990**). ''High intensity narwhal clicks,'' in *Sensory Abilities of Cetaceans*, edited by J. Thomas and R. Kastelein (Plenum, New York), pp. 295–304.

Møhl, B., Wahlberg, M., Madsen, P. T., Miller, L. A., and Surlykke, A. (**2000**). ''Sperm whale clicks: Directionality and source level revisited,'' J. Acoust. Soc. Am. **107**(1), 638–648.

Møhl, B., Wahlberg, M., and Heerfordt, A. (**2001**). ''A GPS-linked array of independent receivers for bioacoustics,'' J. Acoust. Soc. Am. **109**(1), 434–437.

Møhl, B., Madsen, P. T., Wahlberg, M., Au, W. W. L., Nachtigal, P. N., and Ridgway, S. R. (**2003**). ''Sound transmission in the spermaceti complex of a recently expired sperm whale calf,'' ARLO **4**(1), 19–24.

Norris, K. S., and Harvey, G. W. (**1972**). ''A theory for the function of the spermaceti organ of the sperm whale,'' NASA **SP-262**, 397–417.

Oelschläger, H. A., and Kemp, B. (**1998**). ''Ontogenesis of the sperm whale brain,'' J. Comp. Neurol. **399**, 210–228.

Schenkkan, E. J., and Purves, P. E. (**1973**). ''The comparative anatomy of the nasal tract and the function of the spermaceti organ in the *Physeteridae (Mammalia, Odontoceti)*,'' Bijdragen tot de Dierkunde **43**, 93–112.

Schmidt, P. F. (**1954**). ''Further measurements of the sound scattering properties of several marine organisms,'' Deep-Sea Res. **2**, 71–79.

Spiesberger, J. L., and Wahlberg, M. (**2002**). ''Probability density functions for hyperbolic and isodiachronic location,'' J. Acoust. Soc. Am. **112**(6), 3046–3052.

Thode, A., Mellinger, D. K., Stienessen, S., Martinez, A., and Mullin, K. (**2002**). ''Depth-dependent acoustic features of diving sperm whales (*Physeter macrocephalus*) in the Gulf of Mexico,'' J. Acoust. Soc. Am. **112**(1), 308–321.

Urick, R. J. (**1983**). *Principles of Underwater Sound* (McGraw-Hill, New York).

Wahlberg, M. (**2002**). ''The acoustic behaviour of diving sperm whales observed with a hydrophone array,'' J. Exp. Mar. Biol. Ecol. **281**, 53–62.

Wahlberg, M., Lettevall, E., and Medlund, L. (**1995**). ''Estimating the length of sperm whales from interpulse intervals in the clicks,'' Eur. Res. Cetaceans **9**, 38–40.

Wahlberg, M., Møhl, B., and Madsen, P. T. (**2001**). ''Estimating source position accuracy of a large-aperture hydrophone array for bioacoustics,'' J. Acoust. Soc. Am. **109(1)**, 397–406.

Watkins W. A. (**1980**). ''Acoustics and the behavior of sperm whales,'' in *Animal Sonar Systems*, edited by R. G. Busnel and J. F. Fish (Plenum, New York), pp. 283–289.

Watkins, W. A., and Schevill, W. E. (**1977**). ''Spatial distribution of *Physeter catodon* (sperm whales) underwater,'' Deep-Sea Res. **24**, 693–699.

Weilgart, L., and Whitehead, H. (**1988**). ''Distinctive vocalizations from mature male sperm whales (*Physeter macrocephalus*),'' Can. J. Zool. **66**, 1931–1937.

Whitney, W. (**1968**). ''Observations of sperm whale sounds from great depths,'' Marine Physical Laboratory, Scripps Institute of Oceanography No. 1–9. MPL-U-11/68.